Expanding the Space Surveillance Network with Space-Based Sensors Using Metaheuristic Optimization Techniques

Cameron Harris [*]
Virginia Polytechnic Institute and State University
Dylan Thomas[*] **, Jonathan Kadan**[*] **, Dr. Kevin Schroeder**[†]**, Dr. Jonathan Black** [‡]
Virginia Polytechnic Institute and State University

September 2021

ABSTRACT

The increasing congestion of the space domain demands an improvement to space domain/situational awareness capabilities (SDA). Emerging assets to SDA are space-based sensors, which can work in cooperation with the ground-based Space Surveillance Network (SSN) to mitigate coverage gaps and improve state estimates for resident space objects. This work uses a genetic algorithm to perform metaheuristic optimization of potential space-based sensor expansions to the ground-based SSN. Solutions will vary in cost and performance, and some may have benefits or drawbacks not captured in the metaheuristic optimization process. Thus, the results will warrant analysis and discussion.

1. ACRONYMS/ABBREVIATIONS

GEO - Geosynchronous Earth Orbit

HEO - High Earth Orbit

LEO - Low Earth Orbit

MEO - Medium Earth Orbit

RMS - Root Mean Square

RPO - Rendezvous and Proximity Operations

RSO - Resident Space Object

SDA - Space Domain Awareness

SOSI - Space Object Surveillance and Identification

SSN - Space Surveillance Network

2. INTRODUCTION

The rapid proliferation of space-faring nations has turned the near-Earth space domain into a congested and contested frontier. The diverse set of actors, interests, technologies, and objects in Earth orbit has made space domain awareness (SDA) an important objective for ensuring the continued safety of the space domain and its assets. Moreover, the proliferation of space debris and evasive satellites underscores the need for enhanced SDA to maintain tactical awareness of space.

The vast majority of dedicated SDA assets are optical telescopes and radar sensors stationed on Earth. However, recent interest has emerged for space-based sensors performing and maintaining SDA. Space-based sensors provide many advantages, such as dynamic fields of view relative to the Earth's surface and views of orbiting objects unobstructed

[*]Graduate Research Assistant, Kevin T. Crofton Department of Aerospace and Ocean Engineering
[†]Research Scientist, Hume Center for National Security and Technology
[‡]Professor, Kevin T. Crofton Department of Aerospace and Ocean Engineering

Copyright © 2021 Advanced Maui Optical and Space Surveillance Technologies Conference (AMOS) – www.amostech.com

by the atmosphere. Precise state estimation of resident space objects (RSO's) is important for an array of activities in orbit, including sensitive rendezvous and proximity operations, mission characterization, debris removal, and catalog maintenance.

Given continued interest in maintaining tactical SDA, space-based sensors are a compelling asset as a constituent to a SOSI network. However, the design space for both space-based sensor hardware and sensor orbits is vast and complicated. Metaheuristic optimization techniques can be used to traverse the sensor design space, provided there are suitable objective functions to evaluate the performance of space-based sensor design. Previous work in information-based sensor tasking can provide a measure of sensor performance relevant to SDA, as seen in References [13, 12, 20, 14]. Sensor network tasking against a catalog of RSO's extracts useful information about a sensor's ability to observe targets and estimate their states. Combining information-based sensor tasking with metaheuristic optimization, it is possible to formulate performant space-based sensor constellation design for the imminent future of SDA.

3. BACKGROUND

3.1 Space-Based SDA

There have been small, test-sized efforts to introduce surveillance sensors into orbit to perform SDA. The first space-based sensor mission was the Space Based Visible (SBV) sensor, which flew on Mid-Course Space Experiment mission, described in Reference [18]. The SBV operated for 12 years, primarily collecting on GEO RSO's for catalog maintenance for the SSN. The successor to the SBV is the Space-Based Surveillance System (SBSS) program, for which the SBSS-1 satellite has been placed in orbit since 2010.

The history of space-based surveillance efforts have been overall successful, resulting in spin-offs of additional space SDA assets, such as the GSSA. Space-based sensors provide a unique benefit in the fact that they have a view of RSO's unobstructed by atmospheric effects. The utility of space-based assets for SDA has been recognized for years, and some designs for SDA spacecraft constellations have already been proposed, such as Reference [2].

A conclusive effort to add many dedicated space-based assets to the SSN has not yet been finalized. However, given both the need for space-based sensors, as well as the success of the space-based target tracking, it is likely that serious consideration will be made for adding more space-based sensors for SDA in the future.

3.2 SOSI Network Optimization

A SOSI network can be effectively tasked to track a catalog of targets using an information-based tasking strategy. As described in References [15, 20], a tool has been developed to use information-based tasking to simulate a SOSI network tasked to observe a population of RSO's. The measurement data from each independent sensor in the simulated SOSI network is synthesized in the tool to generate state estimates and covariances for the configured RSO's.

For example, a model of the current ground-based Space Sensor Network (SSN) is mapped in Figure 1. The geographical locations of the sensors displayed in Figure 1 are detailed in Table 4.

The geographical distribution of sensors depicted in Figure 1 reveals many gaps in ground-sensor coverage in the Southern Hemisphere and in some eastern meridians. Space-based sensors circumvent the technological limitations or political pitfalls that ground-based sensors face in areas of deep oceans, harsh climates, or unstable geopolitics.

Metaheuristic optimization provides a balance of local search and stochastic exploration, beneficial for traversing complicated non-convex solution spaces. A multi-objective metaheuristic optimizer is well-suited for SOSI network optimization because the design space for space-based sensors is vast and complicated. Moreover, it is important to consider multiple objectives when assessing the performance of a SOSI network, as there is no overarching metric that sufficiently quantifies a SOSI network's quality. Instead, the state estimate data produced from SOSI network simulation is largely up to interpretation. Some basic interpretation of estimate data is provided in the proceeding analysis to perform optimization on a SOSI network using metaheuristic techniques.

4. METHODOLOGY

The present methodology extends the metaheuristic optimization techniques of references [10, 22, 23] to incorporate space-based sensors into an arbitrary distribution of ground-based sensors. The combination of ground-based and

Copyright © 2021 Advanced Maui Optical and Space Surveillance Technologies Conference (AMOS) – www.amostech.com

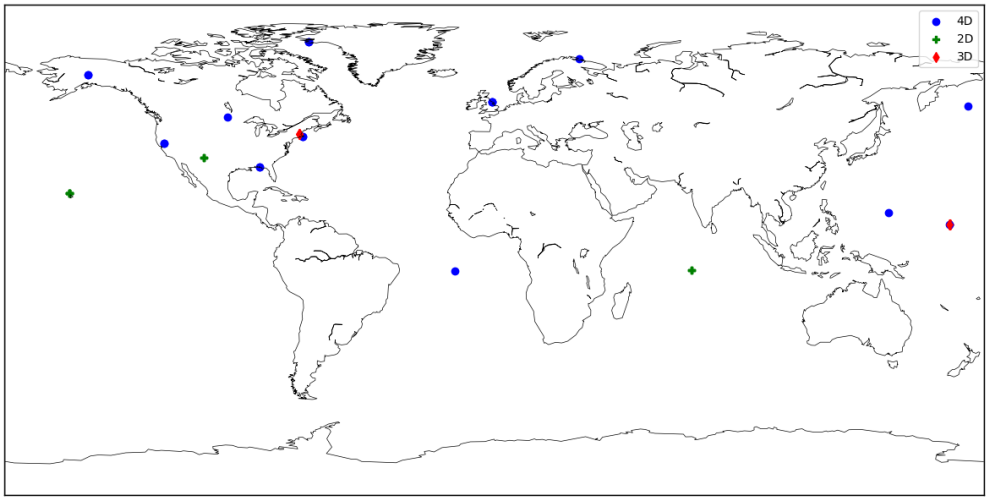

Fig. 1: Current Space Sensor Network: 2D sensors measure AZEL (Azimuth-Elevation), 3D sensors measure AZEL and range, 4D sensors measure AZEL, range, and range-rate.

space-based sensors is referred to as a single SOSI network, and the each SOSI network is subject to centralized tasking.

The metaheuristic optimization of the space-based sensors is performed with a genetic algorithm. The genetic algorithm with a random sampling of solution candidates from the admissible design space, where each solution candidate is a network featuring some amount of space-based sensors complementing the SSN ground-based network. The algorithm iterates over generations of solution candidates until a set of non-dominated candidates is formed. Each generation features a set of 50 solution candidates that are evaluated against a predefined set of optimization objectives to assess the fitness of each candidate. To assess the fitness of a candidate, the associated network is simulated in a test scenario where the network is tasked to maintain state estimates on a catalog of RSO's.

At the termination of a generation, the candidates are stochastically crossed-over and mutated. In the context of the present research, stochastic cross-over or mutation may be a swap or change in orbital parameters or sensor specifications. The logical flow of the optimization process for the SOSI networks is visualized in Figure 2.

The methodology is designed to scale to large catalog of targets to demonstrate real-world applicability. The selected sensor tasking strategy is a Naive, Myopic tasker using Kullback-Leibler divergence as the information reward, as described in Reference [8]. Because the selected network performance objectives are dependent on the tasked observations, it is important to use a scenario where the population of targets is not biased; specifically, the distribution of targets in orbital regimes and orbital characteristics is chosen such that the proportions of targets in the scenario are statistically similar to the known catalog of targets in the real world.

4.1 Test Scenario

An example scenario is needed to test a ground- and space-based SOSI network for its performance. The selected test scenario runs 24 hours at 5 minute timesteps, featuring a set of 252 RSO's in heterogeneous orbital regimes. A 24 hour scenario ensures that LEO and MEO targets will make many revolutions around the Earth, traversing several areas of sparse coverage by the ground-based network. The scenario also ensures that each meridian will experience a full day-night cycle, which is a full visibility cycle for GEO targets.

While a 24 hour scenario does not exhaustively explore tasking opportunities, this is counteracted by the large scope of the RSO catalog. A single day scenario was chosen to ensure the timely delivery of results to demonstrate the capability of this methodology. However, a longer scenario can easily be implemented for a specific use-case as needed.

In the test scenario, the initial estimates on the target catalog are assumed to be good. The application used to demonstrate the methodology is formulated as an expansion of the the current United States SSN using space-based sensors

Copyright © 2021 Advanced Maui Optical and Space Surveillance Technologies Conference (AMOS) – www.amostech.com

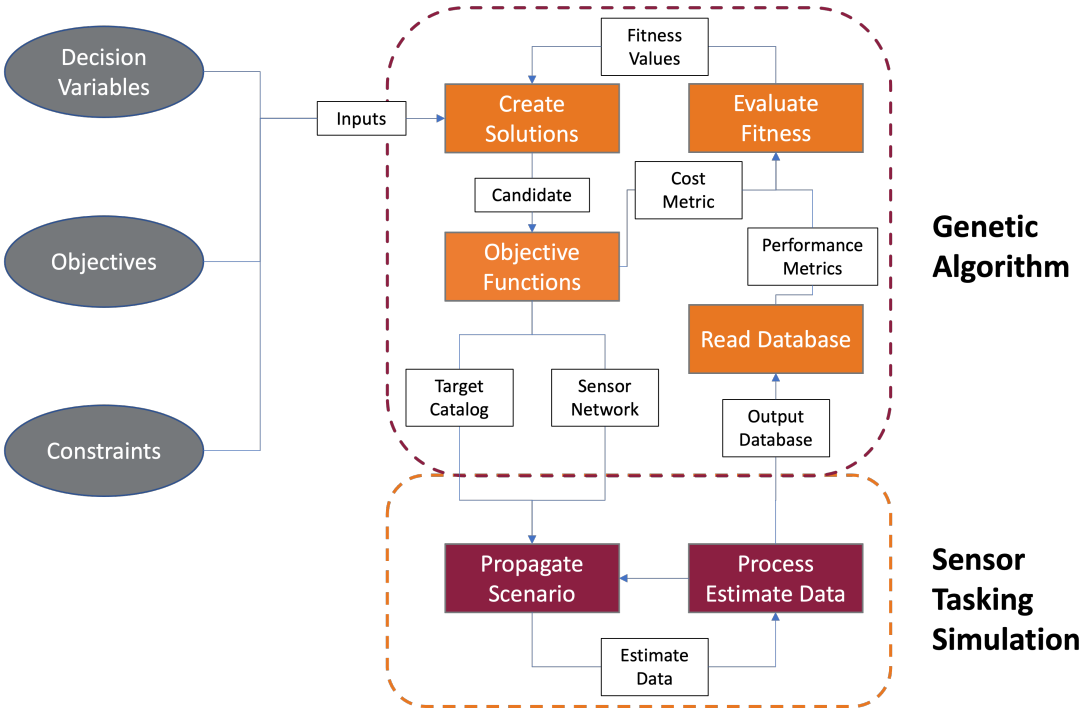

Fig. 2: Sensor Network Optimization Flowchart

to enhance SDA. All space-based sensors are tasked in cooperation with the SSN. As unobserved target states evolve over time, estimates degrade until a sensor is tasked to observe the target. The present application explores how target estimates can be improved when leveraging space-based sensors to track the current catalog, not to search or seek out new targets.

4.2 Decision Variables

The optimization design space allows for the selection of space-based sensor orbits as well as the specifications of the sensors aboard the satellites performing SDA. The exact decision variables for the design space are elaborated on in the subsequent subsections.

4.2.1 Orbit Selection

The current work assumes that space-based sensors will be passive, in that SDA satellites will not actively maneuver to targets to perform observations. Instead, orbits are selected so the space-based sensors will be positioned to collect on targets in a way that prioritizes network performance.

Space-based sensors are generated in sets of Walker-Delta constellations for the computational simplicity and wide coverage. The Walker-Delta constellations may be generated in a maximum of 3 planes, with up to 3 satellites per plane. The exact admissible space for all orbit decision variables in described in Table 1.

4.2.2 Sensor Selection

The space-based sensors are designed as monolithic systems. Each system comes equipped with communications and ADCS subsystems, which are included in the cost calculations. Two options for the sensors are proposed for the present application: an inexpensive option for low-resolution observations, and an expensive option for high-resolution observations. Solutions candidates are formulated as combinations of Walker-Delta constellations, where each constellation consists of satellites hosting one type (i.e., expensive or inexpensive) of sensor. The space-based sensors can slew at a rate of $5^\circ/s$, with an observation efficiency of 0.98.

Copyright © 2021 Advanced Maui Optical and Space Surveillance Technologies Conference (AMOS) – www.amostech.com

Table 1: Orbit Characteristics

Parameter	Admissible Values
Number of Planes	1-3
Satellites Per Plane	1-3
Walker Phasing	0-20°
Semimajor Axis	200-36000 $[km]$
Eccentricity	0.0001-0.1
Inclination	0-100°

Table 2: Expensive Electro-Optical Sensor Characteristics

Parameter	Value	Units
Mass	400	kg
Diameter	304.8	cm
Aperture Area	7.30	m^2
Azimuth Range	$\begin{bmatrix} 0.0 & 2\pi \end{bmatrix}$	$\begin{bmatrix} rads & rads \end{bmatrix}$
Elevation Range	$\begin{bmatrix} 0.0 & \frac{\pi}{2} \end{bmatrix}$	$\begin{bmatrix} rads & rads \end{bmatrix}$
Exemplar	$\begin{bmatrix} 0.00143 & 32500 \end{bmatrix}$	$\begin{bmatrix} m^2 & km \end{bmatrix}$

An expensive sensor system is proposed as one sensor option for demonstration because powerful sensors are useful for resolving distant GEO objects. The expensive sensor is based loosely off the Hubble ACS hardware, described in References [4, 3, 6, 11]. The full list of specifications used to model the expensive sensor are displayed in Table 3.

The inexpensive sensor is proposed to explore the viability of microsatellites for SDA. The inexpensive sensor is based loosely off the Planet Skysat imagery hardware, outlined in References [9, 16, 25]. The inexpensive sensor telescope specifications are modelled after the RC telescope found in Reference [19]. The full list of specifications used to model the inexpensive sensor are displayed in Table 3.

For both sensor types, the exemplar parameter is used to back out the angular resolution of the sensor. The first element of the exemplar is the visible cross-section of a target; the second element of the exemplar is the distance at which the sensor can resolve the visible cross-section. The exemplar used for the inexpensive sensor system is the ground sample distance of the Planet SkySat.

All sensors options are electro-optical, consistent with the current space domain awareness practices with space-based sensors. However, it would be trivially easy to extend the methodology to include radar technology in future work for space-based tracking of orbiting targets.

4.3 Optimization Objectives

The objectives of the optimization process are chosen to weigh the performance of a network against its cost. For initial demonstration, multiple metrics are used to characterize the network's performance towards maintaining SDA, and these SDA metrics are evaluated against the cost of producing the associated constellations of space-based sensors. To characterize a network's performance, some metrics averaged across the target catalog are considered. For instance, the average RMS position error, average Mahalanobis distance, and average observations per target over the target catalog were considered (see Reference [1] for additional information about the Mahalanobis distance).

Copyright © 2021 Advanced Maui Optical and Space Surveillance Technologies Conference (AMOS) – www.amostech.com

Table 3: Inexpensive Electro-Optical Sensor Characteristics

Parameter	Value	Units
Mass	0.09	kg
Diameter	35	cm
Aperture Area	7.065	cm^2
Azimuth Range	$\begin{bmatrix} 0.0 & 2\pi \end{bmatrix}$	$\begin{bmatrix} rads & rads \end{bmatrix}$
Elevation Range	$\begin{bmatrix} 0.0 & \frac{\pi}{2} \end{bmatrix}$	$\begin{bmatrix} rads & rads \end{bmatrix}$
Exemplar	$\begin{bmatrix} 1 & 500 \end{bmatrix}$	$\begin{bmatrix} m^2 & km \end{bmatrix}$

The RMS position error of the i^{th} target at some time t is

$$\varepsilon_{i,RMS}(t) = \sqrt{3} * |\hat{x}_i(t) - x_i(t)| \tag{1}$$

where $|\hat{x}_i(t) - x_i(t)|$ is the Euclidean norm of the position residual of the i^{th} target at time t.

The average RMS position error of the catalog at that time is then:

$$\varepsilon^{AVG}_{RMS}(t) = \frac{\sum_{n=1}^{n_{RSO}} \varepsilon^{n}_{RMS}(t)}{n_{RSO}} \tag{2}$$

where n_{RSO} is the total number of RSO's. For the present demonstration, $n_{RSO} = 252$.

The Mahalanobis distance D of the position estimate on the i^{th} target at some time t is:

$$D_i(t) = \sqrt{(\hat{x}_i(t) - x_i(t))^T S_i^{-1} (\hat{x}_i(t) - x_i(t))} \tag{3}$$

where S_i^{-1} is the inverse position covariance of the i^{th} target at time t.

The average observations per target, O_{AVG}, at some time t is computed as:

$$O_{AVG}(t) = \frac{\sum_{i=1}^{n_{RSO}} n_{i,OBS}(t)}{n_{OBS}(t)} \tag{4}$$

where $n_{i,OBS}(t)$ is the number of observations on the i^{th} target at time (t) and $n_{OBS}(t)$ is the total number of observations made at time t.

All metrics are averaged over the 24 hour scenario in post-processing. The time averages of Eqs 2, 3, and 4 are the objective functions used as demonstration to quantify the performance of a SOSI network.

However, any number of metrics based on estimate error, covariance, or observation number can be used as the network performance objectives for the optimization algorithm. Specific objectives can include observation error or amount of observations on specific high-value targets, number of observations made by a specific sensors, or even observations of a specific sensor made on a specific target. The following metrics are presented as general measures of an arbitrary network tasked against a catalog targets, where all targets are assumed to be equal priority.

The cost associated with a solution is determined by the space-based sensors used in the scenario. Satellite costs are considered individually, but there is a learning rate associated with the sensor technology. The cost of the satellite constellations is computed using the NASA Instrument Cost Model (NICM) presented in the Space Mission Analysis and

Copyright © 2021 Advanced Maui Optical and Space Surveillance Technologies Conference (AMOS) – www.amostech.com

Design text (see Reference [24]). The NICM accounts for subsystem costs as well as launch, fuel, and maintenance. All costs are presented to a rough order of magnitude, and are highly conservative estimates.

Mass and power estimates related to cost are derived from previously existing technology, assumed to be available at a reasonable technology readiness level and high degree of design completeness. The sensor camera and telescope subsystems are considered unique, so development costs are not considered more than once.

It is important to note that the absolute cost of a sensor network addition is not the focus of this research. It is reasonable to assume launch costs, hardware costs, and development costs are all subject to change in the future, especially given the increasing private and government interest in space assets. The utility of a cost model is that it captures the costs of systems or procedures relative to each other. The important focal point of cost estimation in the genetic algorithm is the relative cost of different solutions, which should scale similarly if more nuance is applied to the cost estimation.

Again, the cost modeling used in the solution evaluation largely relies on conservative approximations. For instance, the SDA satellites are assumed to be launched individually, which may not be realistic for large constellations of lower mass satellites, such as the inexpensive satellites considered in this study. The genetic algorithm compares the costs of different solutions, so the relative cost of a solution is more important in the fitness analysis than the absolute cost of a given solution. Higher fidelity cost modeling can be implemented as needed, but highly-specific cost estimation not necessary to get an approximate idea of solutions that provide good performance at a competitive price.

4.4 Computation

Initial computation was performed on a single node, with sequential evaluations of candidate fitness. Each candidate required about 90 minutes to evaluate when computing with a single node. Therefore, evaluating a single generation of solution candidates took several days. Convergence to a Pareto front was infeasible on this timescale.

Recent developments allowed for the genetic algorithm to leverage super-computing to significantly speed up computation time and evaluate all solution candidates simultaneously. Computation of the genetic algorithm was supported by Virginia Tech's Advanced Research Computing (ARC) super-computing resources. Each generation requests 50 nodes for 50 tasks, at 16 cores per task. Therefore, each generation requires about 1 hour of total computation time on a supercomputer, or 800 supercomputer core-hours.

5. EXAMPLE APPLICATION RESULTS

An important result not showed in the final generation is that many initial generations featured solutions with high expenditures (100$B+) resulting in lots of observations, but failed to reduce the average error of the target set significantly. This result underscores the need for not just many satellites performing SDA operations, but rather a strategic set of well-positioned satellites for maintaining SDA of an entire RSO catalog. By considering the average error of the target set, rather than the number of observations (or total coverage), the algorithm ensures that the produced solutions have real-world relevance to SDA.

The genetic algorithm ran for 80 generations with 50 solution candidates in each generation. As noted in Section 4.4, computation time was a limiting factor in algorithm performance. Given the large design space and computational expense, 80 generations are difficult to visualize on a single Pareto front. Based on a similar study in Reference [5], it is reasonable to presume the algorithm solutions would converge to a refined Pareto front with additional time and resources. Leveraging batch requests for super-computing resources, computation time is significantly reduced, and future studies can use supercomputers to refine solutions further. The desired final generation of solutions should contain candidates which are all non-dominated, forming the Pareto front in multiple dimensions. The 80 generations of candidates allowed for demonstration did not comprehensively survey the design space, and therefore not all solutions were non-dominated.

Despite challenges from computation time, solution evolution over several generations revealed interesting niche behavior. Figure 3 compares the semimajor axis selection for solutions in the final generation that opted for 1, 2, and 3 Walker-Delta constellations of SDA spacecraft, respectively. Noticeably, the algorithm showed greatest preference for MEO orbits.

Constellation inclinations were grouped in ranges for clarity. Satellites were considered to be in "low" inclinations for inclinations less than 25°. "Medium" inclinations were considered to range from 25°to 55°. "High" inclinations encompassed 55°to 80°, and "Polar" inclinations were groups beyond 80°.

Copyright © 2021 Advanced Maui Optical and Space Surveillance Technologies Conference (AMOS) – www.amostech.com

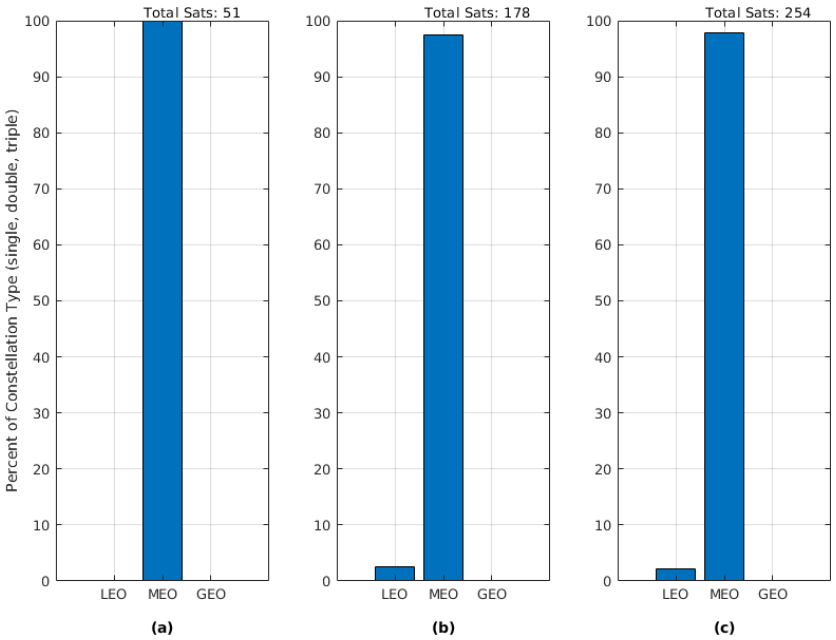

Fig. 3: Population Semimajor Axes for solutions with (a): One Constellation, (b): Two Constellations, (c): Three Constellations

The final generation featured constellations that were predominantly in medium-to-high inclination orbits. The inclination groupings for solutions containing 1, 2, and 3 Walker-Delta constellations, respectively, are shown in Figure 4.

The genetic algorithm showed great preference for the expensive, Hubble-like sensor for its SDA spacecraft; only 10% of the solutions in the final generation featured the lower cost sensors. While the algorithm opted to place nearly all sensors in MEO orbits (almost all between altitudes of $10,000 - 20,000km$), the different sensor types performed fundamentally different tasks for the SOSI network.

Unobstructed by atmospheric effects, high-resolution sensors in MEO orbit can resolve GEO targets with less error than ground-based sensors. Consequently, solutions that opted for the higher cost sensors predominantly tasked the higher cost sensors on the data-sparse GEO targets. The higher cost sensors were tasked to make observations at nearly every available timestep. Many of the expensive space-based sensors were tasked on GEO RSO's in more than 95% of all observations, with occasional HEO targets intermixed. This is likely because the information gain provided by a space-based sensor observation is far greater than a measurement from a ground-based sensor. Not only does a ground-based sensor have to resolve RSO's through the atmosphere, but also the GEO RSO's are potentially tens of thousands of kilometers closer to the space-based sensors. This result is consistent with the goals of the SBV and SBSS missions mentioned in Section 3.1.

Interestingly, the lower cost sensors were primarily tasked on spacecraft in Molniya orbits, such as Molniya-3 and Meridian satellites. With a ground sampling distance of only one meter at $500km$ altitude, it is likely that the lower cost sensors in MEO could not resolve RSO's in GEO orbits. However, the algorithm found a niche for the lower cost space-based sensors for observing Molniya orbits. The model SSN mapped in Figure 1 shows gaps in sensor coverage over eastern meridians, which is the perigee location for Russian spacecraft in Molniya orbits. It is likely the ground-based network constituents could not make comparably valuable observations on Molniya spacecraft during the test scenario, and instead offloaded the observations for the inexpensive space-based sensors. Overall, the lower cost sensors were tasked at infrequent intervals compared to the higher cost sensors.

The niche behavior demonstrated by space-based sensors is not present when tasking a pure ground-based network of sensors. While ground-based optical sensors do tend to be tasked on GEO targets more often, the task separation

Copyright © 2021 Advanced Maui Optical and Space Surveillance Technologies Conference (AMOS) – www.amostech.com

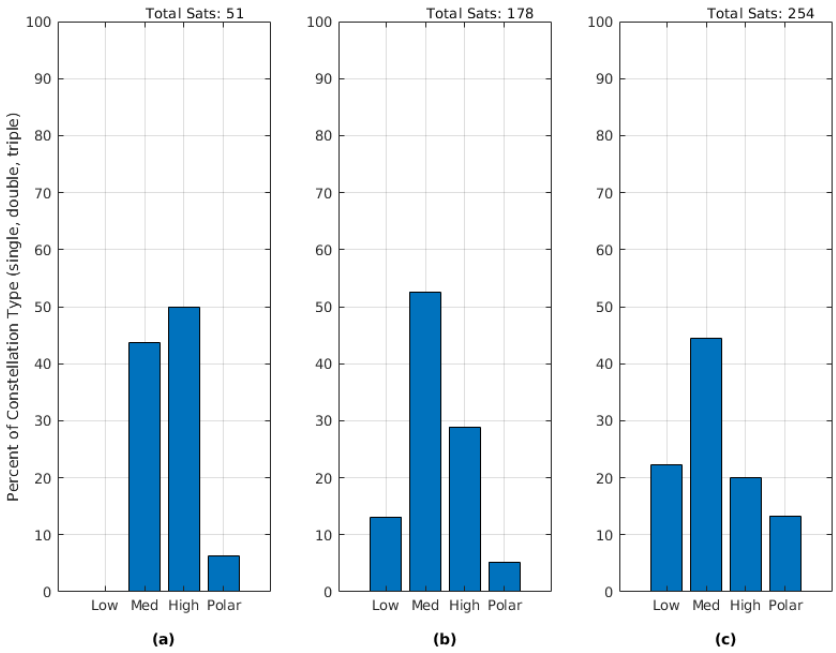

Fig. 4: Population Inclination for solutions with (a): One Constellation, (b): Two Constellations, (c): Three Constellations

between orbital regimes is not as pronounced as SOSI networks using high-resolution space-based sensors.

Figure 5 shows a near linear correlation between space-based sensor constellation cost and the average observations per target. This result is not unexpected, as more greater numbers of spacecraft performing SDA should collect more observations.

Figure 6 shows the final generation fitness values for Average RMS Position Error vs Cost, split between the higher and lower cost sensors. The algorithm's preference for the higher cost sensor constellations shows many data points approaching a Pareto front in the upper plot. The sparse availability of data for the lower cost sensor constellations shows inconclusive development of a Pareto front.

Future investigations will require greater nuance with state error propagation through time, as the steady position state error for frequently-observed RSO's was larger than the starting error for the initial population. Consequently, lower cost solutions that acquired fewer observations returned greater fitness for average position error.

Generally, the standard SSN averaged about 33 observations per target against the set of 252 RSO's used in the test scenario. The average of all solutions in the final generation was about 43 observations per target, a gain of about 10%. Specifically, solutions with 3 Walker-Delta constellations attained an average of 52 observations per target, while solutions with two or one Walker-Delta constellation attained averages of 43 and 36 observations per target, respectively. However, the average cost of a three Walker-Delta constellation solution was double the average cost of a two Walker-Delta constellation, and five times greater than the average cost of a single Walker-Delta constellation of SDA spacecraft.

6. CONCLUSION

The capability demonstrated in this study shows that metaheuristic optimization is a viable method to design space-based assets for supporting SDA. The results suggest that budget microsatellites may not be feasible for maintaining large catalogs of RSO's, but high resolution space-based sensors can support many valuable collections on GEO targets. Information-based tasking of SOSI networks with space-based assets shows that spacecraft sensors tend to take on niche tasking behaviors on a subset of orbital regimes (sensor herding), which is consistent with the mission

Copyright © 2021 Advanced Maui Optical and Space Surveillance Technologies Conference (AMOS) – www.amostech.com

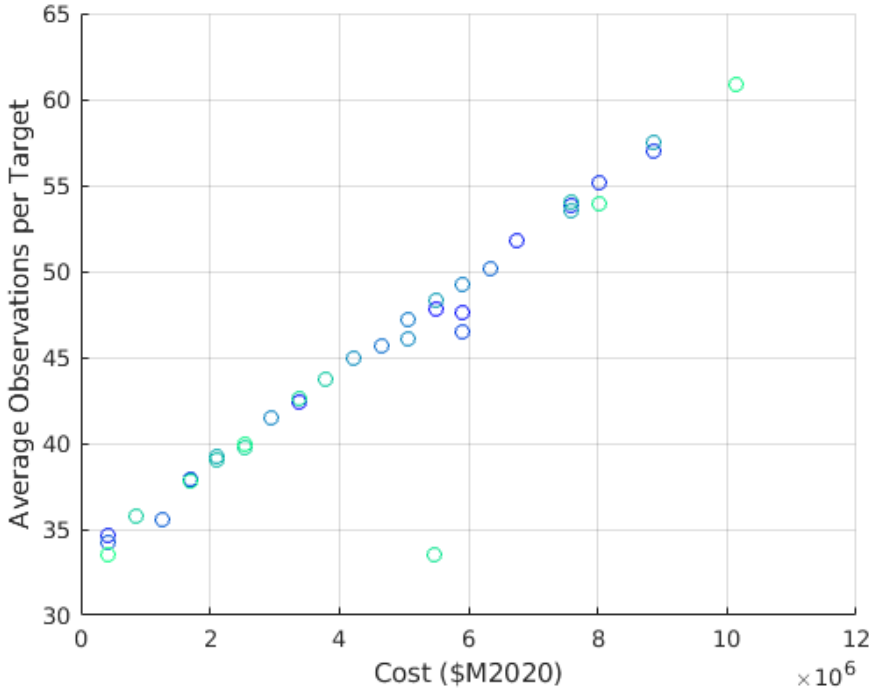

Fig. 5: Average Observations per Target vs Network Cost

objectives of the SBV and SBSS sensor vehicles. Overall, space-based sensors are a compelling asset for SDA, and this research demonstrates that the capability exists to optimize spacecraft sensor design.

7. FUTURE WORK

Imminent future work will be dedicated towards continued computation and formation of the Pareto front for space-based sensors performing SDA. However, the initial investigation has shown interesting results, but future investigations may benefit from a larger design space for the optimization to explore, should computational resources allow. A larger design space could include the options for SDA spacecraft on highly elliptical orbits, alternative constellation configurations, or other types of sensors. Moreover, a larger target catalog coupled with a longer scenario (up to several days, or even weeks) could provide better insight into the performance of a network, though at the cost of great computational expense.

The methodology presented here was designed to be modular and extensible, allowing for straightforward integration with other objectives, constraints, vehicle designs, and cost models. Future investigations with the presented methodology could consider objectives specific to certain high-value targets, or ranked catalogs where not all RSO's have equal priority. A final consideration could be the inclusion of RSO search functionality, where space-based sensors are tasked to not only observe catalogued RSO's, but also search for unobserved RSO's or uncorrelated tracks.

8. ACKNOWLEDGEMENTS

The authors acknowledge Advanced Research Computing at Virginia Tech for providing computational resources and technical support that have contributed to the results reported within this paper. URL: https://arc.vt.edu/

Copyright © 2021 Advanced Maui Optical and Space Surveillance Technologies Conference (AMOS) – www.amostech.com

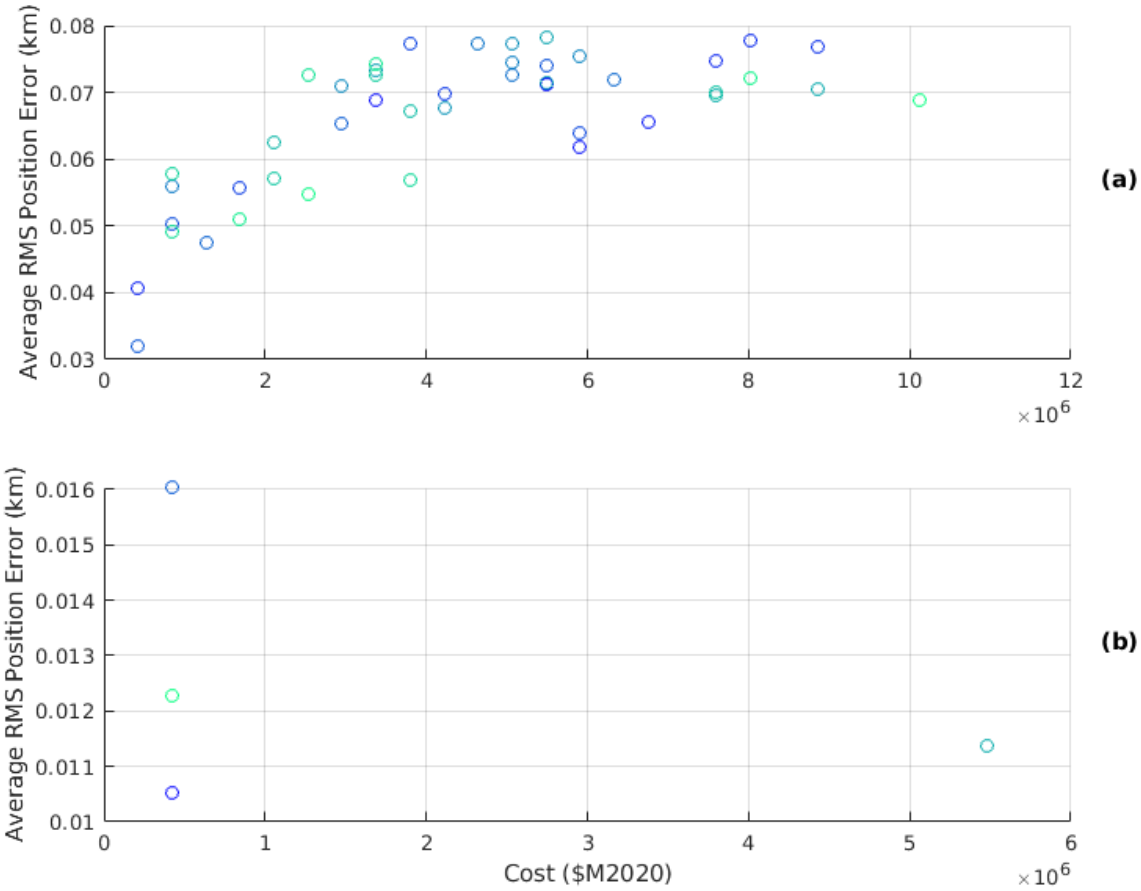

Fig. 6: Pareto front formation for (a): Higher Cost Sensor Constellations, (b): Lower Cost Sensor Constellations

9. APPENDIX

Most sensors in the SSN model are mentioned in Reference [21], but some are elaborated upon in further detail in other sources. All relevant citations are provided in Table 4.

REFERENCES

[1] Roy De Maesschalck, Delphine Jouan-Rimbaud, and Désiré L Massart. The mahalanobis distance. *Chemometrics and intelligent laboratory systems*, 50(1):1–18, 2000.

[2] Jianli Du, Junyu Chen, Bin Li, and Jizhang Sang. Tentative design of sbss constellations for leo debris catalog maintenance. *Acta Astronautica*, 155:379–388, 2019.

[3] ESA. Hubble instruments.

[4] ESA. Hubble's instruments: Acs - advanced camera for surveys.

[5] Cameron D Harris, Jonathan Kadan, Kevin Schroeder, and Jonathan Black. Metaheuristic optimization of a space sensor network distribution. In *ASCEND 2020*, page 4159. 2020.

[6] Space Telescope Science Institute. Acs, 2021.

[7] Nicholas L Johnson. Us space surveillance. *Advances in Space Research*, 13(8):5–20, 1993.

[8] S. Kullback and R. A. Leibler. On information and sufficiency. *The annals of mathematical statistics*, 22(1):79–86, 1951.

Copyright © 2021 Advanced Maui Optical and Space Surveillance Technologies Conference (AMOS) – www.amostech.com

Table 4: Space Surveillance Network

Sensor Name	Sensor Type	Source(s)
Eglin AN/FPS-85 NE	Advanced Radar	[21]
Eglin AN/FPS-85 DS	Advanced Radar	[21, 7]
Globus II AN/FPS-129	Advanced Radar	[21]
Socorro AN/FSD-3 1	Optical	[21]
Socorro AN/FSD-3 2	Optical	[21]
Socorro AN/FSD-3 3	Optical	[21]
Maui AN/FSD-3 1	Optical	[21]
Maui AN/FSD-3 2	Optical	[21]
Maui AN/FSD-3 3	Optical	[21]
Diego Garcia AN/FSD-3 1	Optical	[21]
Diego Garcia AN/FSD-3 2	Optical	[21]
Diego Garcia AN/FSD-3 3	Optical	[21]
BMEWS N AN/FPS-126	Advanced Radar	[21]
BMEWS SE AN/FPS-126	Advanced Radar	[21]
BMEWS SW AN/FPS-126	Advanced Radar	[21]
BMEWS N AN/FPS-123 v7	Advanced Radar	[21]
BMEWS S AN/FPS-123 v7	Advanced Radar	[21]
BMEWS SE AN/FPS-120	Advanced Radar	[21]
BMEWS N AN/FPS-120	Advanced Radar	[21]
Cobra Dane Lower AN/FPS-108	Advanced Radar	[21, 7]
Millstone L-Band	Radar	[21, 7]
Millstone UHF	Radar	[21]
Haystack LRIR	Radar	[21, 17, 7]
Haystack AUX	Radar	[21, 17]
RTS ALCOR	Radar	[21, 7]
RTS ALTAIR UHF	Radar	[21, 7]
RTS ALTAIR VHF	Radar	[21, 7]
RTS MMW	Advanced Radar	[21]
RTS TRADEX	Radar	[21]
MSSS AEOS	Optical	[21]
MSSS BDT	Optical	[21]
MSSS Raven	Optical	[21]
GUAM A SGLS-60	Advanced Radar	[21]
Ascension AN/FPQ-15	Advanced Radar	[21, 7]
PAVE PAWS NE AN/FPS-123	Advanced Radar	[21, 7]
PAVE PAWS SE AN/FPS-123	Advanced Radar	[21, 7]
PAVE PAWS SW AN/FPS-123	Advanced Radar	[21, 7]
PAVE PAWS NW AN/FPS-123	Advanced Radar	[21, 7]
PARCS AN/FPQ-16	Advanced Radar	[21, 7]

[9] Planet Labs. Planet imagery product specifications.

[10] Katherine Mott and Jonathan Black. Model-based heterogeneous optimal space constellation design. In *2018 21st International Conference on Information Fusion (FUSION)*, pages 602–609. IEEE, 2018.

[11] NASA. Fast facts about the hubble space telescope.

[12] Kevin M Nastasi and Jonathan Black. Dynamically tracking maneuvering spacecraft with a globally-distributed, heterogeneous wireless sensor network. In *AIAA SPACE and Astronautics Forum and Exposition*, page 5172, 2017.

[13] Kevin M Nastasi and Jonathan Black. An autonomous sensor management strategy for monitoring a dynamic space domain with diverse sensors. In *2018 AIAA Information Systems-AIAA Infotech@ Aerospace*, page 0890.

Copyright © 2021 Advanced Maui Optical and Space Surveillance Technologies Conference (AMOS) – www.amostech.com

2018.
[14] Kevin M Nastasi and Jonathan T Black. Adaptively tracking maneuvering spacecraft with a globally distributed, diversely populated surveillance network. *Journal of Guidance, Control, and Dynamics*, 42(5):1033–1048, 2019.
[15] Kevin Michael Nastasi. *Autonomous and Responsive Surveillance Network Management for Adaptive Space Situational Awareness*. PhD thesis, Virginia Tech, 2018.
[16] Earth Observation Portal. Skysat constellation of terra bella - formerly skysat imaging program of skybox imaging.
[17] CL Stokely, JL Foster, EG Stansbery, JR Benbrook, and Q Juarez. Haystack and hax radar measurements of the orbital debris environment; 2003. *NASA JSC-62815, November*, 2006.
[18] Grant Stokes, Curt vo, Ramaswamy Sridharan, and Jayant Sharma. The space-based visible program. In *Space 2000 Conference and Exposition*, page 5334, 2000.
[19] Buy Telescopes. Alluna optics alluna rc-16 16" f/8 ritchey chretien telescope.
[20] Dylan J Thomas, Kevin M Nastasi, Kevin Schroeder, and Jonathan T Black. Autonomous multi-phenomenology space domain sensor tasking and adaptive estimation. In *2018 21st International Conference on Information Fusion (FUSION)*, pages 1331–1338. IEEE, 2018.
[21] David A Vallado and Jacob D Griesbach. Simulating space surveillance networks. In *Paper AAS 11-580 presented at the AAS/AIAA Astrodynamics Specialist Conference. July*, 2011.
[22] Katherine M Wagner and Jonathan T Black. Genetic-algorithm-based design for rideshare and heterogeneous constellations. *Journal of Spacecraft and Rockets*, pages 1–12, 2020.
[23] Katherine Mott Wagner. *Optimization of Disaggregated Space Systems Using the Disaggregated Integral Systems Concept Optimization Technology Methodology*. PhD thesis, Virginia Tech, 2020.
[24] James R Wertz, David F Everett, and Jeffery J Puschell. *Space mission engineering: the new SMAD*. Microcosm Press, 2011.
[25] Chengxing Zhai, Michael Shao, Stephen Lai, Paul Boerner, Jonny Dyer, Edward Lu, Harold Reitsema, and Marc Buie. Asteroid detection demonstration from skysat-3 b612 data using synthetic tracking. *arXiv preprint arXiv:1805.01102*, 2018.

Copyright © 2021 Advanced Maui Optical and Space Surveillance Technologies Conference (AMOS) – www.amostech.com